Spintronic Transport through Polyphenoxyl Radical Molecules

Katsunori Tagami* and Masaru Tsukada

Department of Physics, Graduate School of Science, University of Tokyo, 7-3-1 Hongo, Bunkyo-ku, Tokyo 113-0033, Japan

Received: December 20, 2003; In Final Form: March 6, 2004

The coherent quantum transport properties through the spin-polarized polyphenoxyl radical molecule have been investigated, using the density-functional-derived tight-binding model and the Green's functions method. The majority and minority spin components exhibit considerably different transmission spectra in the vicinity of the Fermi level. Namely, each spin component carries a different amount of current when the bias voltage is applied between the two electrodes that sandwich the polyradical molecule. Therefore, if the magnetization axis of the polyradical is fixed by the external magnetic field, and if the spin flip does not occur during the transmission, the assumed molecular bridge is expected to work as a spin filter or a spin valve. Furthermore, as long as the bias voltage is weak, the total spin current is observed to be larger than the current through its reduced molecular form. It indicates that the adsorption of some chemical species on the radical sites can be sensed by the change in conductance of the molecular bridge.

Introduction

Since Rajca et al. developed a synthetic method of organic high-spin polymers,[1−3] π-conjugated magnetic polyradicals have been studied extensively in the research field of organic magnetism. In these molecules, the unpaired electrons on the radical sites are designed to be located in a non-Kekulé and nondisjointed fashion[4] and to interact cooperatively with each other to form the high-spin electronic states. Remarkably, some of them have been reported to be stable even at room temperature.[5−7] Thus, as an industrial application, these organic magnetic molecules are expected as candidates of molecular magnets. On the other hand, in the research field of single-molecular devices, the molecule-dependent quantum transport properties are one of the hot scientific issues, and the demand of synthesizing functional macromolecules is getting higher. Along this line, the transport properties of high-spin polyradical molecules are also attracting attention. However, to our knowledge, the detailed transport properties of the polyradical molecules have not been examined from either the experimental or theoretical viewpoints. Therefore, our intent in this work is to predict their coherent quantum transport properties theoretically.

For this purpose, we consider the molecular bridge structure in which a single polyradical molecule is bridged between two gold electrodes. As an illustrated example, we adopt the poly-(4-phenoxyl-1,2-phenylenevinylene) radical molecule in which the phenylenevinylene-based polymer is substituted with the phenoxyl radicals at the specific sites. Although the number of phenoxyl radicals is restricted to four in this article, we adopt the expression "polyradical" in the following discussions, because the word "oligoradical" is not widely used. In addition, to clarify the effects of the radicals on the transport properties, we calculate not only the transmission spectrum through the polyradical molecule, but also the spectra through the backbone polymer chain itself (i.e., the poly(1,2-phenylenevinylene)) and through the hydrogen-reduced polyradical molecule (i.e., the poly(4-hydroxyphenyl-1,2-phenylenevinylene)).

* Author to whom correspondence should be addressed. E-mail: tagami@cms.phys.s.u-tokyo.ac.jp.

Model and Method

Figure 1a schematically illustrates the molecular bridge where the backbone polymer chain, the poly(1,2-phenylenevinylene), is bridged between two gold electrodes through Au−S bonds. Similarly, Figure 1b and c illustrate the molecular bridges where this polymer molecule is 4-substituted with the hydroxyphenyls and phenoxyl radicals, respectively. The number of radical units is fixed to be four in this paper. In the following discussions, we call these molecules type-A, type-B, and type-C molecules, for simplicity. From a synthetic viewpoint, the type-B molecule is a precursor to achieve the type-C polyradical.

The atomic configuration of these electrode−molecule−electrode system is set in the following way. First, the atomic coordinates of these three types of molecular wires, including two thiol (S−H) bonds at their ends, are optimized by ab initio calculations (Gaussian98), using the B3LYP exchange-correlation functional[8,9] with the LANL2DZ bases.[10−12] These molecules then are assumed to be sandwiched between two gold electrodes semi-infinitely extended along the [110] direction. The electrodes are assumed to have a rodlike structure whose diameters are ∼10 Å, and the ends of the rodlike structures that face the molecules are assumed to have sharp apexes. In making contact with the gold electrodes, H atoms in S−H bonds are assumed to be removed, and thiolate (S−Au) bonds are assumed to be formed instead. The S atoms are located on top of the apex Au atoms of the electrodes. The length of the S−Au bonds is set to ∼2.55 Å.

The electronic states and charge distributions of this type of metal−molecule−metal system are solved by the spin-polarized self-consistent tight-binding model, based on the density functional theory (DFT).[13] This tight-binding formalism has been well-established and has been applied to the research of various materials. For example, it has been successfully applied to inorganic materials, such as silicon surfaces,[14−17] and to organic materials, such as DNA[18,19] and nanotubes,[20] oligoporphyrin molecular wires,[21−24] and benzothiophene-based molecular solenoids.[25] The Hamiltonian and overlap matrixes are expanded by the atomic orbital sets, i.e., the 2s and 2p orbitals for C and O atoms, the 1s orbital for H atoms, the 3s and 3p orbitals for

10.1021/jp037953e CCC: $27.50
Published on Web 04/27/2004

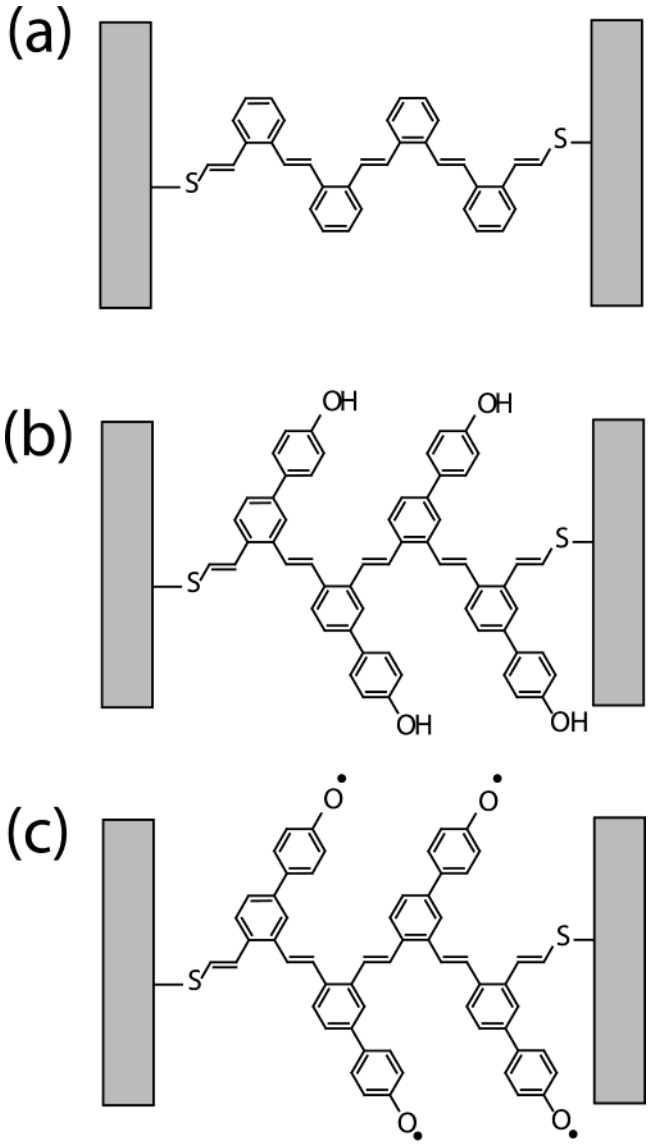

Figure 1. Schematically illustrated molecular bridges. Between the gold electrodes (shaded) are (a) the poly(1,2-phenylenevinylene) backbone chain, (b) its 4-substituted molecule with hydroxyphenyl groups bridged through the Au−S bonds, and (c) its 4-substituted molecule with phenoxyl radicals bridged through the Au−S bonds.

S atoms, and the 5d and 6s orbitals for Au atoms. The on-site levels, and the two-center hopping and overlap integrals, are obtained from the norm-conserving atomic pseudo-potentials and the corresponding pseudo-wave functions, in a manner similar to those reported in ref 13.

To treat the infinite system size, we assume the extended-molecule approach,[26,27] in which the system is divided into three parts, i.e., the left electrode, the scattering region, and the right electrode. Here, the molecules and a fraction of the gold electrodes are considered as the scattering region. Accordingly, the Hamiltonian matrix H_σ is divided into 3×3 sections for each spin component, i.e.,

$$H_\sigma = \begin{pmatrix} H_{\mathrm{L},\sigma} & V_{\mathrm{LM},\sigma} & 0 \\ V^\dagger_{\mathrm{LM},\sigma} & H_{\mathrm{M},\sigma} & V_{\mathrm{RM},\sigma} \\ 0 & V^\dagger_{\mathrm{RM},\sigma} & H_{\mathrm{R},\sigma} \end{pmatrix} \quad (1)$$

where $\sigma = \uparrow,\downarrow$. The overlap matrix S_σ is also divided in a similar manner. The matrix elements that correspond to the intraelectrode interactions $H_{\mathrm{L(R)}}$ and the electrode-scattering region

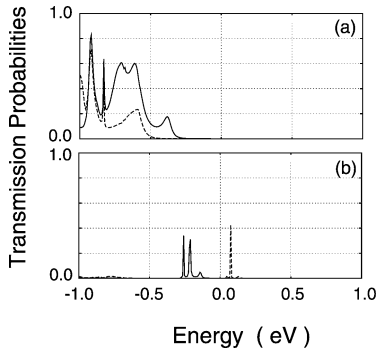

Figure 2. (a) Transmission spectra through type-A (broken line) and type-B molecular bridges (solid line). (b) Transmission spectrum through type-C molecular bridge. The solid and broken lines in panel c correspond to the up and down spin components, respectively.

couplings $V_{\mathrm{LM(RM)},\sigma}$ are used to calculate the Green's functions ($g_{\mathrm{L(R)},\sigma}(z)$) and the self-energy terms ($\Sigma_{\mathrm{L(R)},\sigma}$)[28] at the electrode, i.e.,

$$g_{\mathrm{L(R)},\sigma}(z) = (zS_{\mathrm{L(R)},\sigma} - H_{\mathrm{L(R)},\sigma})^{-1} \quad (2)$$

$$\Sigma_{\mathrm{L(R)},\sigma}(z) = (zS^\dagger_{\mathrm{LM(RM)},\sigma} - H^\dagger_{\mathrm{LM(RM)},\sigma}) g_{\mathrm{L(R)},\sigma}(z) \times (zS_{\mathrm{LM(RM)},\sigma} - H_{\mathrm{LM(RM)},\sigma}) \quad (3)$$

Note here that, because the gold electrodes are assumed to be spin-unpolarized, $H_{\mathrm{L(R)},\uparrow} = H_{\mathrm{L(R)},\downarrow}$ and $g_{\mathrm{L(R)},\uparrow} = g_{\mathrm{L(R)},\downarrow}$. The charge distribution inside the extended molecule is obtained by integrating its Green's function $G_{M,\sigma}$ along the contour on the imaginary plane.[26] The number of grid points on the contour is set to 80. Here, $G_{\mathrm{M},\sigma}$ is defined as

$$G_{\mathrm{M},\sigma}(z) = (zS_{\mathrm{M},\sigma} - H_{\mathrm{M},\sigma} - \Sigma_{\mathrm{L},\sigma} - \Sigma_{\mathrm{R},\sigma})^{-1} \quad (4)$$

The aforementioned calculations are repeated until the self-consistent charge distribution is obtained.[26] After the charge distribution has converged, the transmission spectrum $T_\sigma(E)$ is calculated using the following equation:[26]

$$T_\sigma(E) = 4\mathrm{Tr}[\mathrm{Im}(\Sigma_{\mathrm{L},\sigma}) G_{\mathrm{M},\sigma} \mathrm{Im}(\Sigma_{R,\sigma}) G^\dagger_{\mathrm{M},\sigma}] \quad (5)$$

Results and Discussion

Transmission Spectra. Figure 2a shows the transmission spectra $T_\sigma(E)$ through the spin-unpolarized type-A and type-B molecules, i.e., $T_\uparrow = T_\downarrow$. The broken and solid lines correspond to the spectra of the former and latter molecules, respectively. The horizontal axis corresponds to the electron energy E incident from the electrode, whose origin is set to the Fermi level of the gold electrodes. Here, the Fermi level of the electrodes was determined beforehand by the band structure calculation for the infinitely long gold rods. When the hydroxyphenyl groups are introduced to the backbone chain, the highest occupied peak in the spectra shifts from $E = -0.59$ to $E = -0.38$ eV. Note here that such a peak shift is also observed when the number of hydroxyphenyl group is varied from 1 to 3 by changing the length of the backbone polymer. Therefore, the hydroxyphenyl group is considered to be acting as the electron donor.

The narrow peak width at $E = -0.83$ eV reflects the corresponding charge distributions, which are highly weighed at the gold electrodes. As for the other peaks, the corresponding charge densities are delocalized along the molecules with different weights on the hydroxyphenyl groups and the backbone chain. However, as the molecular structures and their wave

functions have no clear symmetries, further identifications of these peaks with molecular levels are not straightforward.

In contrast, the type-C molecular wire takes the spin-polarized electronic states. (The spin polarization inside the molecule is retained, irrespective of disturbation caused by coupling to the electrodes.[29]) Figure 2b shows the transmission spectra through the type-C wire, where all the spin orientation of the four radicals are aligned. In other words, the type-C molecule is in the quintet state. The solid and broken lines correspond to the transmission spectra of the majority (up) and minority (down) spins, respectively. The splitting of the transmission spectra between both spin components was observed, irrespective of the number of radicals.

Interestingly, both the up and down spin transport channels appear around the Fermi level, which indicates that this molecular bridge is conductive, even at lower bias voltages. Their peak widths are very narrow as the corresponding charge densities are dominantly distributed on the phenoxyl radicals, and their coupling to the electrode wave functions are not strong. In addition, at $-1.1 < E < -0.3$ eV, the transmission amplitudes are found to become very weak (at most 0.016). A similar feature is not observed in the transmission spectra of the type-A and type-B wire (see Figure 2a). It indicates that the influence of extracting the H atoms from OH groups in Figure 1b is not localized around the hydroxyphenyl group, but, instead, it reaches the backbone chain. In fact, the O atoms in the type-C molecule are more negatively charged (by 0.11 e) than those in the type-B molecule. Such a difference in the charge density between both types of molecules is found to survive around the backbone chain, although its absolute value is smaller than that on the radical site. As a result, the transmission spectra of the type-C molecular bridge does not resemble those of the type-B molecular bridge.

Current−Voltage Curves. On the basis of the transmission spectra obtained previously, we predicted their current−voltage ($I-V$) curves, using the equation

$$I(V) = g_0 \sum_{\sigma} \int_{E_F - eV/2}^{E_F + eV/2} T_\sigma(E)\, dE \qquad (6)$$

where $g_0 = e^2/h$ and V is the voltage applied between the two electrodes. Note here that this equation is only valid within the linear response regime, and nonequilibrium calculations with finite bias voltage should be necessary to predict more-accurate $I-V$ curves. However, the $I-V$ curves that are achieved have some attractive points worthy of discussion.

The dotted, broken, and solid lines in Figure 3a correspond to the $I-V$ curves of the type-A, type-B, and type-C molecular bridges, respectively. In this figure, the total spin current, i.e, the summation of the current carried by both spin components, is plotted. The first two molecular bridges show the semiconductive behaviors with the threshold bias voltage of ∼0.7 and 0.4 V for the corresponding cases. The lower threshold bias of the type-B structure originates from its transmission peak, which lies closer to the Fermi level (see Figure 2a). In contrast, the type-C molecular bridge has a very small threshold bias of 0.1 V, which is caused by the transmission peaks around the Fermi level (see Figure 2b). The stepwise shape of the $I-V$ curve reflects the narrowness of the successive peaks around the Fermi level and low transmission amplitudes at $E < -0.3$ eV.

Here, the difference of the $I-V$ curves between the type-B and type-C wires is significant from the viewpoint of their applications, because the current strength can be changed drastically only by reducing the phenoxyl groups in the molecule. Namely, as long as the bias is set to be <0.7 V, the conductance of the molecular bridge will be suppressed after some chemical species adsorb on the radical sites. This observation means that the molecular bridge may work as a chemical sensor. This expectation agrees well with a scanning tunneling microscopy (STM) experiment where the similar polyradical molecules have been observed to be brighter than their reduced molecular forms.[30]

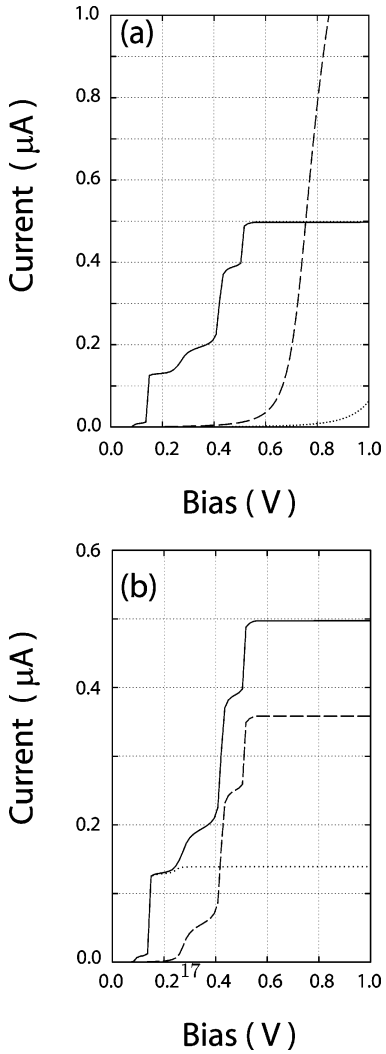

Figure 3. (a) Current−voltage ($I-V$) curves of type-A (dotted line), type-B (broken line), and type-C (solid line) molecular bridges. (b) $I-V$ curves of type-C molecular bridges, where the broken, dotted, and solid lines correspond to the up and down spin components, and their total, respectively.

Spin Current. Finally, we comment on the current strength carried by each spin component. The broken, dotted, and solid lines in Figure 3b correspond to the current by the up and down spin components, and their total, respectively. At $0.1\ V < V < 0.2$ V, the current is carried dominantly by the down spin. At $V > 0.2$ V, the up spin component starts to carry the current, whereas the strength of the down spin current does not change. As the bias increases, the up spin current exceeds the down spin current. When the up spin current saturates at $V = 0.55$ V, its strength is ∼2.58 times as large as the down spin current. Note that these phenomena originate from the asymmetry of the transmission spectra between the two spins around the Fermi level.

From the viewpoint of applications, it is very attractive that the molecular bridges can transport each spin component with different weights, although the electrodes themselves are spin-

unpolarized. For example, if the magnetization axis of the polyradical is fixed by the external magnetic field, and if the spin flip does not occur during the transmission, the assumed molecular bridge is considered to be used as a spin filter or a spin valve. Such a function may be observed in a more dramatic manner, when the spin-polarized (ferromagnetic) electrodes are adopted.[31,32] This point should be clarified in future works.

Conclusions

In conclusion, the quantum transport properties through a spin-polarized phenylenevinylene-based polyradical molecule—the poly(4-phenoxyl-1,2-phenylenevinylene) radical—in the coherent transport regime have been investigated using the density-functional-derived self-consistent tight-binding model and the Green's functions method. We found that the majority and minority spin components show considerably different transmission spectra in the vicinity of the Fermi level. Namely, each spin component carries a different amount of current when the bias voltage is applied between the two electrodes that sandwich the molecule. Therefore, if the magnetization axis of the polyradical is fixed by the external magnetic field, and if the spin flip does not occur during the transmission, the assumed molecular bridge is expected to work as a spin filter or a spin valve. Furthermore, as long as the bias voltage is <0.7 V, the total spin current is observed to be larger than the current through its reduced molecular form. This observation indicates that the adsorption of some chemical species on the radical sites can be sensed by the change in the conductance of the molecular bridge.

Acknowledgment. This work was supported in part by the Ministry of Education, Culture, Sports, Science and Technology, Grant-in-Aid for Creative Scientific Research "Devices on Molecular and DNA Levels". The authors thank to Prof. H. Nishide, Mr. T. Iwasaki, and Mr. M. Tanaka for fruitful discussions on the organic magnetism. The numerical calculations were performed on SR8000 at the Computer Center at the University of Tokyo.

References and Notes

(1) Rajca, A.; Wongsriratanakul, J.; Rajca, S.; Cernny, R. *Angew. Chem., Int. Ed.* **1998**, *37*, 1229.
(2) Rajca, A.; Rajca, S.; Wongsriratanakul, J. *J. Am. Chem. Soc.* **1999**, *121*, 6308.
(3) Rajca, A.; Wongsriratanakul, J.; Rajca, S. *Science* **2001**, *294*, 1503.
(4) Nishide, H. *Adv. Mater.* **1995**, *7*, 937.
(5) Miyasaka, M.; Yamazaki, T.; Tsuchida, E.; Nishide, H. *Macromolecules* **2000**, *33*, 8211, and references therein.
(6) Nishide, H.; Ozawa, T.; Miyasaka, M.; Tsuchida, E. *J. Am. Chem. Soc.* **2001**, *123*, 5942.
(7) Kaneko, T.; Matsubara, T.; Aoki, T. *Chem. Mater.* **2002**, *14*, 3898.
(8) Becke, A. D. *J. Chem. Phys.* **1993**, *98*, 5648.
(9) Lee, C.; Yang, W.; Parr, R. G. *Phys. Rev. B* **1988**, *37*, 785.
(10) Hay, P. J.; Wadt, W. R. *J. Chem. Phys.* **1985**, *82*, 270.
(11) Wadt, W. R.; Hay, P. J. *J. Chem. Phys.* **1985**, *82*, 284.
(12) Hay, P. J.; Wadt, W. R. *J. Chem. Phys.* **1985**, *82*, 299.
(13) Frauenheim, T.; Seifert, G.; Elstner, M.; Niehaus, T.; Köhler, C.; Amkreutz, M.; Sternberg, M.; Hajnal, Z.; Carlo, A. D.; Suhai, S. *J. Phys.: Condens. Matter* **2002**, *14*, 3015.
(14) Tagami, K.; Tsukada, M. *Surf. Sci.* **2001**, *493*, 56.
(15) Tagami, K.; Sasaki, N.; Tsukada, M. *Appl. Surf. Sci.* **2001**, *172*, 301.
(16) Tagami, K.; Tsukada, M. *Jpn. J. Appl. Phys.* **2000**, *39*, 6025.
(17) Tagami, K.; Sasaki, N.; Tsukada, M. *J. Phys. Soc. Jpn.* **2000**, *69*, 3937.
(18) Reha, D.; Kabelac, M.; Ryjacek, F.; Sponer, J.; Sponer, J. E.; Elstner, M.; Suhai, S.; Hobza, P. *J. Am. Chem. Soc.* **2002**, *124*, 3366.
(19) Tagami, K.; Matsumoto, T.; Kawai, T.; Tsukada, M. *Jpn. J. Appl. Phys.* **2003**, *42*, 5887.
(20) Carlo, A. D.; Gheorghe, M.; Lugli, P.; Sternberg, M.; Seifert, G.; Frauenheim, T. *Physica B* **2002**, *314*, 86.
(21) Tagami, K.; Tsukada, M.; Matsumoto, T.; Kawai, T. *Phys. Rev. B* **2003**, *67*, 245324.
(22) Tagami, K.; Tsukada, M. *Jpn. J. Appl. Phys.* **2003**, *42*, 3606.
(23) Tagami, K.; Tsukada, M. *Curr. Appl. Phys.* **2003**, *3*, 439.
(24) Tagami, K.; Tsukada, M. *e-J. Surf. Sci. Nanotech.* **2003**, *1*, 45. (Available via the Internet at http://www.sssj.org/ejssnt/.)
(25) Tagami, K.; Tsukada, M.; Wada, Y.; Iwasaki, T.; Nishide, H. *J. Chem. Phys.* **2003**, *119*, 7941.
(26) Taylor, J.; Guo, H.; Wang, J. *Phys. Rev. B* **2001**, *63*, 245407.
(27) Xue, Y.; Datta, S.; Ratner, M. A. *J. Chem. Phys.* **2001**, *115*, 4292.
(28) Nardelli, M. B. *Phys. Rev. B* **1999**, *60*, 7828.
(29) Tagami, K.; Wang, L.; Tsukada, M. *Nano Lett.* **2004**, *4*, 2009.
(30) Tanaka, M. Nishide, H., private communications.
(31) Emberly, E. G.; Kirczenow, G. *Chem. Phys.* **2002**, *281*, 311.
(32) Pati, R.; Senapati, L.; Ajayan, P. M.; Nayak, S. K. *Phys. Rev. B* **2003**, *68*, 100407.